ARTICLE

Non-genomic activation of the AKT-mTOR pathway by the mitochondrial stress response in thyroid cancer

Woo Kyung Lee Doolittle[1,8,9], Sunmi Park[2,9], Seul Gi Lee[3], Seonhyang Jeong[2], Gibbeum Lee[4], Dongryeol Ryu[5], Kristina Schoonjans[6], Johan Auwerx[7], Jandee Lee[4]✉ and Young Suk Jo[2]✉

© The Author(s), under exclusive licence to Springer Nature Limited 2022

Cancer progression is associated with metabolic reprogramming and causes significant intracellular stress; however, the mechanisms that link cellular stress and growth signalling are not fully understood. Here, we identified a mechanism that couples the mitochondrial stress response (MSR) with tumour progression. We demonstrated that the MSR is activated in a significant proportion of human thyroid cancers via the upregulation of heat shock protein D family members and the mitokine, growth differentiation factor 15. Our study also revealed that MSR triggered AKT/S6K signalling by activating mTORC2 via activating transcription factor 4/sestrin 2 activation whilst promoting leucine transporter and nutrient-induced mTORC1 activation. Importantly, we found that an increase in ^{mt}DNA played an essential role in MSR-induced mTOR activation and that crosstalk between MYC and MSR potentiated mTOR activation. Together, these findings suggest that the MSR could be a predictive marker for aggressive human thyroid cancer as well as a useful therapeutic target.

Oncogene (2022) 41:4893–4904; https://doi.org/10.1038/s41388-022-02484-7

INTRODUCTION

Metabolic reprogramming is a hallmark of cancer that facilitates macromolecule synthesis and supports increased energy demands, cellular survival, and tumour proliferation [1]. Increased glycolysis and the suppression of mitochondrial oxidative phosphorylation (OXPHOS) were thought to be an essential feature of tumour cell metabolism, as postulated by Warburg [2]. However, cancer cells display metabolic flexibility that allows them to adapt to different metabolic conditions [3–6] via mechanisms that mediate changes in glucose utilization as well as amino acid and lipid metabolism [7]. This metabolic flexibility can also trigger the mitochondrial stress response (MSR), suggesting that the adaptive mechanisms associated with mitochondrial stress, which rely on efficient mito-nuclear communication, are conserved in cancer cells [8–11].

The mitochondrial unfolded protein response (^{mt}UPR) is an important mitochondrial stress pathway that has been investigated extensively in invertebrates such as *Drosophila melanogaster* and *Caenorhabditis elegans* [12]. In these invertebrates, the ^{mt}UPR is activated by mitochondrial proteotoxic stresses, such as unfolded protein accumulation, impaired protein quality control, and OXPHOS inhibition. These stressors co-ordinately induce the transcription of genes encoding chaperones, proteases, and metabolic enzymes that restore mitochondrial function and induce cellular adaptation [12–15]. The mechanisms via which the ^{mt}UPR is activated and integrated with other autonomous or non-autonomous cellular stress responses in vertebrates are currently under intensive research [9].

The integrated stress response (ISR) is a highly conserved intracellular stress pathway that regulates global protein synthesis [16] and can be activated by oxidative, endoplasmic reticulum (ER), mitochondrial, and nutritional stresses [9, 17, 18]. The ISR is initiated by the phosphorylation of the α-subunit of eukaryotic translation initiation factor 2 (eIF2α) by kinases including general control non-derepressible 2 (GCN2) and PKR-like ER kinase (PERK). Phosphorylated eIF2α then suppresses global protein synthesis while specifically promoting the expression of stress-response genes, such as activating transcription factor 4 (ATF4), thereby inducing various stress proteins that restore cellular homoeostasis [18–20]. However, cell-based experiments have been unable to provide a clear mechanistic link between the MSR and autonomous proliferative signalling, which is a hallmark of cancer [21, 22].

Mechanistic target of rapamycin (mTOR) is a master kinase regulator of metabolic signalling that integrates environmental cues for cellular growth and stimulates the *de novo* synthesis of cellular building blocks [23]. Previous studies have shown that mitochondrial stress rapidly inhibits the mTOR signalling pathway, thereby reducing cytosolic protein translation and cell

[1]Laboratory of Molecular Biology, Center for Cancer Research, National Cancer Institute, National Institutes of Health, Bethesda, MD 20892, USA. [2]Department of Internal Medicine, Open NBI Convergence Technology Research Laboratory, Yonsei University College of Medicine, Seoul 03722, South Korea. [3]Department of Surgery, Eulji University School of Medicine, Daejeon 34824, South Korea. [4]Department of Surgery, Open NBI Convergence Technology Research Laboratory, Yonsei Cancer Center, Severance Hospital, Yonsei University College of Medicine, Seoul 03722, South Korea. [5]Laboratory of Molecular and Integrative Biology, Department of Molecular Cell Biology, Sungkyunkwan University School of Medicine, Suwon 16419, South Korea. [6]Laboratory of Metabolic Signaling, École Polytechnique Fédérale de Lausanne, Lausanne 1015, Switzerland. [7]Laboratory of Integrative Systems Physiology, École Polytechnique Fédérale de Lausanne, Lausanne 1015, Switzerland. [8]Present address: Department of Medicine, University Hospitals Cleveland Medical Center, Case Western Reserve University, Cleveland, OH 44106, USA. [9]These authors contributed equally: Woo Kyung Lee Doolittle, Sunmi Park. ✉email: jandee@yuhs.ac; joys@yuhs.ac

Received: 2 May 2022 Revised: 18 September 2022 Accepted: 22 September 2022
Published online: 4 October 2022

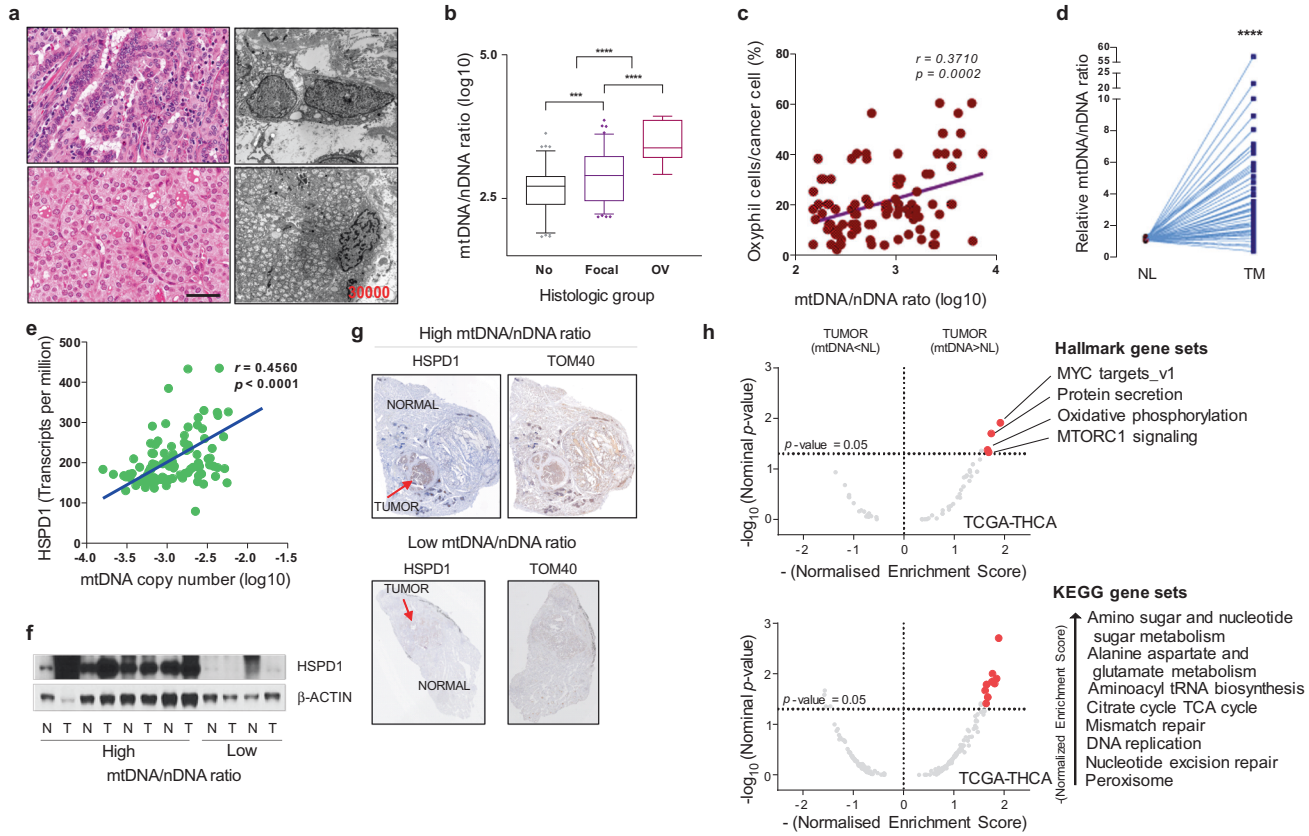

Fig. 1 ^{mt}DNA copy number, ^{mt}UPR, and mTOR signalling in thyroid cancer. a Microscopic findings of classical PTC (upper) and ovPTC (lower). Scale bar = 25 µm. Magnification = ×30,000 for electron microscopy. **b** Comparison of ^{mt}DNA/^{n}DNA ratio according to oxyphil cell number. No = no oxyphil cell ($n = 99$). Focal ≤ 70 % oxyphil cells ($n = 98$). OV ≥ 70% oxyphil cells ($n = 11$). **c** Relationship between ^{mt}DNA/^{n}DNA ratio and oxyphil cell number in focal tumours ($n = 98$). **d** Comparison of ^{mt}DNA/^{n}DNA ratio between PTC and NL from the same patients ($n = 53$). PTC showed no oxyphil cells. **e** Relationship between mtDNA copy number and *HSPD1* mRNA expression (transcripts per million) in TCGA-THCA (PTC, $n = 100$). **f** Representative results of western blotting analysis using tissue samples from patients with non-ovPTC. N indicates paired normal thyroid tissues while T indicates tumour tissues. **g** Representative IHC-P staining images of tissue samples from PTC with high or low ^{mt}DNA/^{n}DNA ratios. TOM40, a component of the mitochondrial outer membrane, was used as a mitochondrial marker. **h** Enriched Hallmark and KEGG genes ($p < 0.05$, FDR $q < 0.25$) in high ^{mt}DNA copy number tumours from TCGA-THCA. ***$p < 0.001$, ****$p < 0.0001$. Data represent the mean ± SD. PTC papillary thyroid cancer, ^{mt}DNA mitochondrial DNA, ^{n}DNA nuclear DNA, OV oncocytic variant, NL matched normal tissues, TM tumour, HSPD1 heat shock protein family D member 1 (HSP60), TOM40 translocase of outer mitochondrial membrane 40, IHC-P immunohistochemistry-paraffin-embedded tissues.

proliferation [24, 25]. However, the mTOR pathway is activated in animal models of mitochondrial disease [26, 27] and aberrant mTOR signalling is a feature of the MSR during senescence and aging [28, 29]. In cancer cells, genetic and genomic alterations are thought to govern PI3K/AKT/mTOR signalling regardless of mitochondrial stress; however, The Cancer Genome Atlas (TCGA) has suggested that genetic and genomic alterations in this pathway occur at a lower frequency than expected [30–33]. Thus, maintaining metabolic flexibility in cancer cells may require dynamic interactions between signalling molecules rather than fixed genetic alterations.

Unfortunately, it has been difficult to identify dynamic non-genomic alterations in signalling pathways using clinical tissue samples due to confounding variables like diverse driver gene mutations and concomitant genomic instability within an already complex signalling system [34–36]. To overcome this problem, we analysed the role of MSR and the mechanism coupling the MSR to mTOR signalling in a cohort of patients from The Cancer Genome Atlas Thyroid Cancer (TCGA-THCA), since thyroid cancers harbour homogenous driver mutations and have a lower somatic mutation and genetic alteration burden than other solid tumours [33, 37, 38]. Together, our findings suggest that the MSR could be a predictive marker for aggressive human thyroid cancer as well as a useful therapeutic target.

RESULTS

Mitochondrial DNA (^{mt}DNA) copy number is linked to ^{mt}UPR and mTOR signalling in human thyroid cancer

Aerobic glycolysis is a key feature of cancer cells that induces mitochondrial stress [39]. The compensatory response of cancer cells to this mitochondrial stress can facilitate their invasion, metastasis, and drug resistance [40, 41]. A subset of thyroid cancers contains oxyphil cells with an increased number of mitochondria, also known as Hurthle or Askanazy cells. Human papillary thyroid carcinoma (PTC) with >70% oxyphil cells is defined as oncocytic type PTC (ovPTC) and has a poor prognosis. Here, we found that the number of mitochondria was increased in a subset of cancers, resulting in oxyphil cells with many mitochondria (Fig. 1a). Although not as extensive as in ovPTC, there were some cases with focal oxyphil changes and focal increases in the number of mitochondria, as reflected by an increased ^{mt}DNA copy number (Fig. 1b, c). Furthermore, cancer cells had more ^{mt}DNA than matched normal cells (Fig. 1d), even though no oxyphil changes were observed. A high ^{mt}DNA copy number was also associated with poor prognosis in our non-ovPTC and TCGA-THCA cohorts (Tables 1 and 2, Supplementary Tables 1 and 2). As this increase in ^{mt}DNA might induce mito-nuclear imbalance in protein translation leading to ^{mt}UPR, the expressions of genes related to ^{mt}UPR, including six chaperone genes, six

Table 1. Clinicopathological characteristics in non-ovPTC according to ^{mt}DNA/^{n}DNA ratio ($n = 197$).

	^{mt}DNA/^{n}DNA ratio		*P* value
	Lower third (<2.56) ($n = 64$) (%)	**Upper third (>2.96) ($n = 72$) (%)**	
mtDNA/nDNA ratio, log10 (IQR)[††]	2.33 (2.11–2.45)	3.24 (3.05–3.46)	<0.001*
Age (years), median (IQR)	38 (28–56)	48 (36–59)	0.010*
BMI (kg/m$^{2)}$, median (IQR)	22.7 (20.0–25.6)	24.3 (22.2–27.3)	0.006*
Gender (female)	48 (75.0)	51 (70.8)	0.586[†]
Tumour size (cm), median (IQR)	1.5 (1.1–2.1)	1.7 (1.2–2.3)	0.241*
MACIS score, median (IQR)	4.2 (3.6–5.1)	4.9 (4.4–6.7)	0.002*
Histological subtype			
Follicular variant	13 (20.3)	17 (23.6)	0.253[†]
Conventional	51 (79.7)	51 (70.8)	
Solid variant	0 (0.0)	2 (2.8)	
Tall cell variant	0 (0.0)	2 (2.8)	
Bilaterality			
Negative	46 (71.9)	53 (73.6)	0.820[†]
Positive	18 (28.1)	19 (26.4)	
Extrathyroidal extension			
No	36 (56.3)	21 (29.2)	0.001[†]
Yes	28 (43.8)	51 (70.8)	
T stage			
T1	31 (48.4)	19 (26.4)	0.066[†]
T2	3 (4.7)	4 (5.6)	
T3	25 (39.1)	40 (55.6)	
T4	5 (7.8)	9 (12.5)	
N stage			
N0	17 (26.6)	24 (33.3)	0.390[†]
N1	47 (73.4)	48 (66.7)	
M stage			
M0	62 (96.9)	72 (100.0)	0.131[†]
M1	2 (3.1)	0 (0.0)	
TNM stage[ʃ]			
I/II	48 (75.0)	35 (48.6)	0.002[†]
III/IV	16 (25.0)	37 (51.4)	
BRAF^{V600E} mutation			
Absent	31 (48.4)	16 (22.2)	0.001[†]
Present	33 (51.6)	56 (77.8)	
TERT promoter mutation			
Absent	63 (98.4)	69 (95.8)	0.370[†]
Present	1 (1.6)	3 (4.2)	

MACIS distant Metastasis, patient Age, Completeness of resection, local Invasion, and tumour Size.
**p* values calculated using an independent *t*-test or Mann–Whitney *U* test. Data are expressed as the mean (IQR).
[†]*p* values calculated using a χ^2 test or linear-by-linear association.
[††]*IQR* interquartile range.
[ʃ]T-, N-, M-, TNM- stage according to the AJCC TNM staging system 7[e].

Table 2. Multivariate analysis of the association of high third ^{mt}DNA copy number with high-risk clinicopathological and molecular parameters in non-ovPTC.

	^{mt}DNA copy number (upper third)		
	Odds ratio	**95% CI**	***P* value**
Age (≥45)			
Model A	2.337	1.172–4.662	0.016
Model B	2.506	1.243–5.052	0.010
Model C	2.542	1.241–5.204	0.011
Model D	2.431	1.157–5.110	0.019
Model E	2.114	0.985–4.538	0.055
BRAF^{V600E} mutation (present)			
Model F	2.962	1.392–6.304	0.005
Model G	2.846	1.328–6.097	0.007
Model H	2.855	1.332–6.122	0.007
Model I	2.840	1.292–6.242	0.009
Model J	2.478	1.103–5.568	0.028
Extrathyroidal extension (present)			
Model F	2.955	1.430–6.107	0.003
Model G	2.827	1.359–5.879	0.005
Model H	2.857	1.370–5.961	0.005
Model K	2.799	1.325–5.912	0.007
Model L	2.806	1.307–6.023	0.008
TNM stage (stage III/IV)			
Model A	3.167	1.524–6.580	0.002
Model B	2.983	1.424–6.246	0.004
Model C	3.137	1.454–6.767	0.004
Model D	3.050	1.383–6.729	0.006
Model E	2.458	1.084–5.574	0.031

Model A: Adjusted for gender.
Model B: Adjusted for gender and BMI (≥25).
Model C: Adjusted for gender, BMI, and MACIS score (≥7).
Model D: Adjusted for gender, BMI, MACIS score, and extrathyroidal extension.
Model E: Adjusted for gender, BMI, MACIS score, extrathyroidal extension, and BRAFV600E mutation.
Model F: Adjusted for age at diagnosis and gender.
Model G: Adjusted for age at diagnosis, gender, and BMI.
Model H: Adjusted for age at diagnosis, gender, BMI, and MACIS score.
Model I: Adjusted for age at diagnosis, gender, BMI, MACIS score, and extrathyroidal extension.
Model J: Adjusted for age at diagnosis, gender, BMI, MACIS score, extrathyroidal extension, and TNM stage.
Model K: Adjusted for age at diagnosis, gender, BMI, MACIS score, and TNM stage.
Model L: Adjusted for age at diagnosis, gender, BMI, MACIS score, TNM stage, and BRAF^{V600E} mutation.

proteases, four mitokines, and nine other related genes, were compared between normal and tumour tissues using TCGA-THCA [42]. As shown in Supplementary Fig. 1, many genes related to ^{mt}UPR such as heat shock protein family D (Hsp60) member 1 (HSPD1), TNF receptor associated protein 1 (TRAP1), prohibitin 1 (PHB1), prohibitin 2 (PHB2), caseinolytic mitochondrial matrix peptidase proteolytic subunit (CLPP), lon peptidase 1, mitochondrial (LONP1), lon peptidase 2, peroxisomal (LONP2), OMA1 zinc metallopeptidase (OMA1), and growth differentiation factor 15 (GDF15) were upregulated. To select a representative marker related to ^{mt}DNA copy number among those genes related to ^{mt}UPR, multiple correlation analyses were performed. We

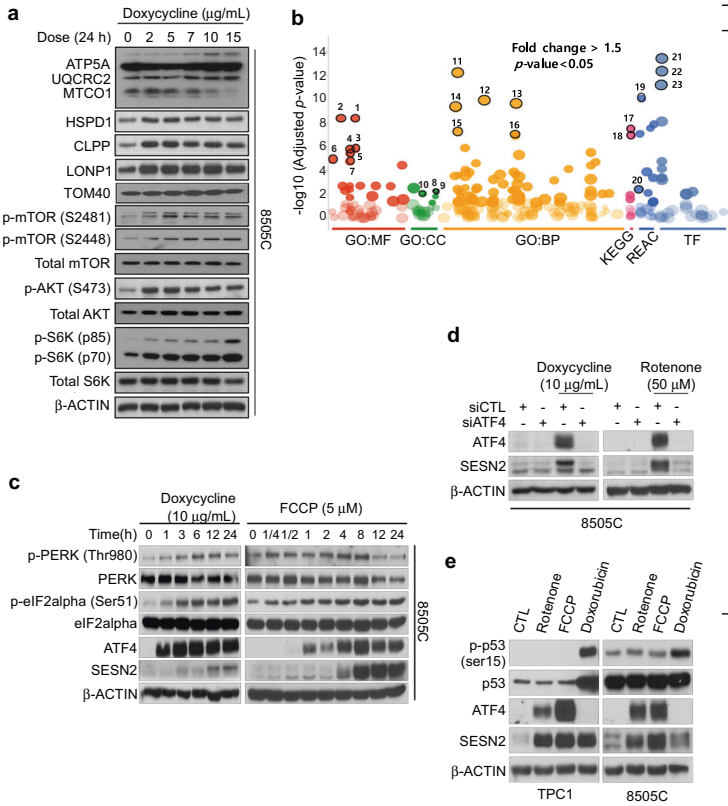

No.	Source	Term ID	Term name
1	GO:MF	GO:0016875	ligase activity, forming carbon-oxygen bonds
2	GO:MF	GO:0004812	aminoacyl-tRNA ligase activity
3	GO:MF	GO:0016874	ligase activity
4	GO:MF	GO:0015179	L-amino acid transmembrane transporter activity
5	GO:MF	GO:0015175	neutral amino acid transmembrane transporter activity
6	GO:MF	GO:0000049	tRNA binding
7	GO:MF	GO:0015171	amino acid transmembrane transporter activity
8	GO:CC	GO:1990617	CHOP-ATF4 complex
9	GO:CC	GO:1990184	amino acid transport complex
10	GO:CC	GO:0038201	TOR complex
11	GO:BP	GO:0006520	cellular amino acid metabolic process
12	GO:BP	GO:0019752	carboxylic acid metabolic process
13	GO:BP	GO:0043436	oxoacid metabolic process
14	GO:BP	GO:0006082	organic acid metabolic process
15	GO:BP	GO:0006418	tRNA aminoacylation for protein translation
16	GO:BP	GO:0043039	tRNA aminoacylation
17	KEGG	KEGG:00970	Aminoacyl-tRNA biosynthesis
18	KEGG	KEGG:01230	Biosynthesis of amino acids
19	REAC	REAC:R-HSA-379716	Cytosolic tRNA aminoacylation
20	REAC	REAC:R-HSA-381119	Unfolded Protein Response (UPR)
21	TF	TF:M09869	Factor: ATF-4; motif: RNMTGATGCAAY
22	TF	TF:M09839	Factor: ATF4; motif: ATTGCATCAT
23	TF	TF:M08199	Factor: ATF-4:TEF; motif: GGMTGATGCAATM

Fig. 2 ^{mt}UPR is closely related to the integrated stress response for mTOR signalling activation. a OXPHOS, mtUPR marker, and mTOR signalling protein expression and phosphorylation in doxycycline-treated 8505C cells. **b** Transcriptome analysis of doxycycline-treated 8505C cells showing significantly enriched GO, KEGG, Reactome (REAC), and transcription factor (TF) terms. **c** Doxycycline and FCCP induce the integrated stress response, ATF4, and SESN2 in 8505C cells. **d** ATF4 silencing affects SESN2 induction by doxycycline and rotenone. Immunoblots represent at least three independent experiments. **e** ATF4/SESN2 activation in FCCP- or rotenone-induced mitochondrial stress or in doxorubicin-induced genotoxic stress in TPC1 and 8505C cells. Immunoblots represent at least three independent experiments. OXPHOS oxidative phosphorylation, ATP5A ATP synthase F1 subunit alpha, UQCRC2 ubiquinol-cytochrome C reductase core protein 2, MTCO1 mitochondrially encoded cytochrome C oxidase I, HSPD1 heat shock protein family D member 1, CLPP mitochondrial matrix peptidase proteolytic subunit, LONP mitochondrial lon peptidase 1, TOM40 translocase of outer mitochondrial membrane 40, S6K ribosomal protein S6 kinase, PERK PKR-like ER kinase (eukaryotic translation initiation factor 2 alpha kinase 3, EIF2AK3), eIF2α α-subunit of eukaryotic translation initiation factor 2, ATF4 activating transcription factor 4, SESN2 sestrin 2, CTL control, FCCP carbonyl cyanide-4-(trifluoromethoxy) phenylhydrazone.

observed that 18 out of 25 genes showed positive correlations with ^{mt}DNA copy number and of these, 11 were statistically significant (Fig. 1e and Supplementary Fig. 2). Among these 11 genes, HSPD1 and TRAP1 had the highest correlation. HSPD1 was selected as the representative ^{mt}UPR marker because HSPD1 has higher expression value (transcripts per million) and has been widely used in experiments [15]. This finding was confirmed by the western blotting analysis using tissue samples (Fig. 1f) and immunohistochemical (IHC) staining of paraffin-embedded tissue samples (IHC-P; Fig. 1g, Supplementary Fig. 3a–e). In addition, gene set enrichment analysis (GSEA) was conducted to confirm the representativeness of HSPD1 as a ^{mt}UPR marker. The expression of other ^{mt}UPR markers was also enriched in PTC samples with high *HSPD1* expression, indicating that HSPD1 could be a marker of ^{mt}UPR (Supplementary Fig. 3f).

To understand the molecular features of PTC with a high ^{mt}DNA copy number, we divided PTC samples into groups with high and low ^{mt}DNA copy numbers compared to matched normal tissues. In PTC with a high ^{mt}DNA copy number, Hallmark gene sets related to MYC targets, protein secretion, OXPHOS, and mTOR signalling were highly enriched, as were KEGG gene sets related to amino acid metabolism (Fig. 1h, Supplementary Tables 3 and 4). Gene set enrichment analysis (GSEA) of our transcriptomic data according to HSPD1 expression also indicated the enrichment of MYC targets, protein secretion, OXPHOS, mTOR signalling, and UPR Hallmark gene sets (Supplementary Fig. 4a, Supplementary Table 5). GSEA also revealed the enrichment of KEGG gene sets related to aminoacyl tRNA biosynthesis, ribosomes, and thyroid cancer (Supplementary Fig. 4b, Supplementary Table 6). Consistently, GSEA of TCGA-THCA revealed that the upregulated gene sets were similar to those in our transcriptome data (Supplementary Fig. 4c, d, Supplementary Tables 7 and 8). Together, these results suggest that mitochondrial stress pathways and genes related to the MSR may be co-ordinately upregulated in PTC with high ^{mt}DNA copy number. Moreover, the MSR may be linked to mTOR signalling and amino acid metabolism.

ATF4/SESN2 upregulation by mitochondrial stress

To verify the biological function of MSR induced by a high ^{mt}DNA copy number, we treated human thyroid cancer cell lines, such as BCPAP, TPC1, C643, and 8505C, with doxycycline, which induces ^{mt}UPR and inhibits mitochondrial translation [15]. Consistent with previous reports [43], doxycycline downregulated MTCO1, upregulated HSPD1, and increased the secretion of growth differentiation factor 15 (GDF15), a stress-inducible mitokine, in HeLa cells (Supplementary Fig. 5a). The same effects were observed in 8505C thyroid cancer cells treated with doxycycline, but not amoxicillin (Supplementary Fig. 5b). In addition, doxycycline increased the expression of mitochondrial matrix peptidase proteolytic subunit (*CLPP*) and mitochondrial lon peptidase 1 (*LONP1*; Fig. 2a), while

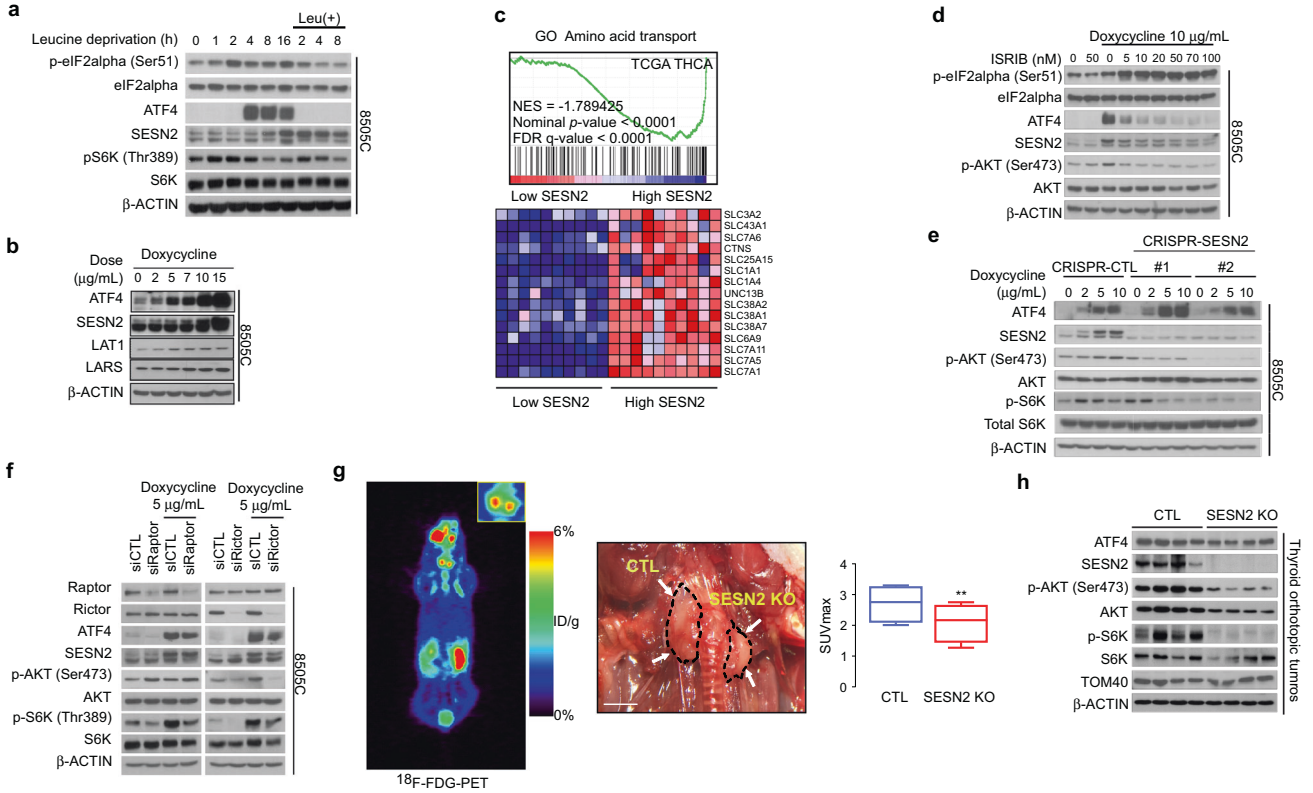

Fig. 3 Dual mechanism via which MSR maintains mTOR activity. a Effect of leucine supplementation on ATF4/SESN2 expression and S6K (Thr389) phosphorylation in leucine-deprived 8505C cells. Immunoblots represent at least three independent experiments. **b** Coordinated enrichment of amino acid transport-related genes in tumours with high *SESN2* expression. **c** LARS and LAT1 protein expression in doxycycline-treated 8505C cells. **d** ISRIB affects ATF4/SESN2 and AKT (Ser473) phosphorylation induced by doxycycline in 8505C cells. **e** *SESN2* knockout affects AKT (Ser473) and S6K (Thr389) phosphorylation induced by doxycycline. **f** *Raptor* or *Rictor* silencing affect AKT (Ser473) and S6K (Thr389) phosphorylation induced by doxycycline in 8505C cells. **g** Representative image of orthotopic thyroid tumours, corresponding ^{18}F-FDG-PET results, and SUV_{max} between CRISPR-CTL and CRISPR-SESN2-KO tumours ($n = 7$/group) of the right and left thyroid of the same mouse (arrows). *p* values calculated using Wilcoxon matched-pairs signed rank tests. **h** ATF4 and SESN2 expression and AKT (Ser473) and S6K (Thr389) phosphorylation in CRISPR-CTL and CRISPR-SESN2-KO orthotopic tumours. Immunoblots represent at least three independent experiments. $^{**}p < 0.01$. Data represent the mean ± SD. LARS leucyl-tRNA synthetase, LAT1 L-type amino acid transporter 1, ISRIB integrated stress response inhibitor, SUV_{max} maximum standardised uptake value, CTL control, KO knockout.

increasing mTOR, AKT, and S6K phosphorylation, suggesting AKT-mTOR signalling activation (Fig. 2a).

To clarify the mechanistic link between ^{mt}UPR and mTOR, we performed transcriptome analysis using doxycycline-treated 8505C cells, finding that doxycycline induced ATF4 transactivation and increased amino acid metabolism (Fig. 2b). Consistent with previous data [18], these findings suggest that ^{mt}UPR is closely associated with the ISR, as evidenced by increased PERK and eIF2α phosphorylation with ATF4 and SESN2 induction (Fig. 2c). SESN2, a known ATF4 target under mitochondrial dysfunction, has dual actions as a leucine (Leu)-dependent mTORC1 inhibitor and mTORC2 activator through direct interaction with GATOR2-mTORC2 [44–46]. By silencing ATF4 in 8505 C cells treated with doxycycline and rotenone, a mitochondrial complex I inhibitor that can also be used as a mitochondrial stress inducer, we revealed that SESN2 induction was dependent on ATF4 (Fig. 2d). In BCPAP (B-Raf Proto-Oncogene, Serine/Threonine Kinase (BRAF)^{V600E} positive PTC) cells, doxycycline concomitantly induced ATF4 and SESN2 (Supplementary Fig. 5c), while rotenone induced ATF4/SESN2 in TPC1 PTC cells (Supplementary Fig. 5c). FCCP, a mitochondrial OXPHOS uncoupling agent used as a mitochondrial stress inducer, also activated the ISR (Supplementary Fig. 5d, left panel) and increased AKT and S6K phosphorylation before appearance of cleaved caspase and poly(ADP-ribose) polymerase (PARP), indicating cellular apoptosis (Supplementary Fig. 5d, right panel). These data suggest that the ^{mt}UPR is coupled with ISR induction and mTOR signalling via ATF4/SESN2. Notably, doxorubicin also induced SESN2 without ATF4 induction in TPC1 cells, but not in 8505C cells which harbour a p53 mutation (Fig. 2e), suggesting that SESN2 is also induced by genotoxic stress via a p53-dependent pathway. Thus, SESN2 upregulation by genotoxic stress requires p53, but that induced by mitochondrial stress requires ATF4. Taken together, these data demonstrate that mitochondrial stress is linked to signalling pathways related to biosynthesis and cell proliferation, potentially via ATF4/SESN2.

Amino acid metabolism is closely linked to the MSR

Since SESN2 is a Leu sensor that can inhibit mTORC1 activation by interacting with the GATOR2 complex [47, 48], the MSR could negatively affect cancer cell proliferation. Although TCGA-THCA revealed significant *SESN2* upregulation, *SESN3* was downregulated (Supplementary Fig. 6a). Consistent with an association between the ^{mt}UPR and ATF4-SESN2, we found that *SESN2* expression correlated positively with *HSPD1* and *ATF4* (Supplementary Fig. 6b, c) and that HSPD1, ATF4, and SESN2 had similar IHC staining patterns (Supplementary Fig. 6d). In addition, we found a strong positive correlation between *HSPD1, ATF4, SESN2*, and *GDF15* (Supplementary Fig. 7a). Therefore, we removed Leu from the culture medium of 8505C cells to determine whether SESN2 inhibited mTORC1 (Fig. 3a). Increased eIF2α and decreased S6K phosphorylation suggested nutritional stress and mTORC1 inactivation, respectively; however, adding Leu to the medium

abolished eIF2α phosphorylation and restored S6K phosphorylation, even in the presence of SESN2 (Fig. 3a). Thus, SESN2 does not appear to inhibit mTORC1 under Leu-rich conditions.

Since the GSEA of doxycycline-treated 8505C cells indicated that the MSR is linked to amino acid metabolism (Fig. 2b) and correlation analysis revealed that the MSR is related to cellular amino acid biosynthesis rather than amino acid catabolism (Supplementary Fig. 7b, c), we investigated whether cancer cells generate Leu-rich conditions during the MSR. Doxycycline activated the MSR by inducing leucyl-tRNA synthetase 1 (LARS) and L-type amino acid transporter 1 (LAT1), which regulates the cellular uptake of large neutral amino acids (leucine, methionine, and valine; Fig. 3b). Consistently, *LARS* and methionyl-tRNA synthetase 1 (MARS) were upregulated in tumours with high *HSPD1* expression (Supplementary Fig. 7d, e). Our correlation analysis also indicated that MSR is related to cellular amino acid transporters (Supplementary Fig. 8a). GSEA indicated that genes related to amino acid transport were upregulated in tumours with high *SESN2* expression (PTC-hiSESN2) (Fig. 3c), suggesting the involvement of amino acid transporters. Indeed, the expression of *SLC7A5* and *SLC3A2*, which encode L-type amino acid transporter 1 (LAT1), was significantly higher in tumour samples (Supplementary Fig. 8b) and correlated positively with *SESN2* expression (Supplementary Fig. 8c). Although SESN2 is thought to inhibit mTORC1, our data suggest that the upregulation of amino acid transporters and biosynthesis following the MSR may disable this effect. Considering the positive correlation between *SESN2, LARS*, *SLC7A5*, and *SLC3A2* in TCGA-THCA, we examined whether the MSR upregulates these genes via *ATF4/SESN2*; however, silencing ATF4 did not affect LAT1 and LARS upregulation by the MSR, suggesting that LAT1 and LARS induction do not require ATF4/SESN2 (Supplementary Fig. 8d).

MSR activates mTOR through ISR-ATF4/SESN2 signalling

Our in silico analyses also indicated a relationship between the MSR and cell growth signalling. The PI3K/AKT/mTOR pathway plays a major role in thyroid carcinogenesis by facilitating aggressive tumour behaviour [49–52]. GSEA of Hallmark gene sets indicated that mTORC1 and PI3K-AKT-mTOR signalling was co-ordinately upregulated in PTC-hiSESN2 (Supplementary Fig. 9a, Supplementary Table 9). Consistently, HSPD1, ATF4, and SESN2 expression correlated positively with PI3K-AKT signalling-related genes (Supplementary Fig. 9b). As SESN2 also showed positive correlation with the genes of interest in this study and pS6K(T389) (Supplementary Fig. 9c), we performed in vitro and in vivo experiments to investigate the effect of SESN2 on tumour behaviour. SESN2 overexpression in 8505C and TPC1 cells increased cell proliferation and AKT (Ser473) phosphorylation, providing direct evidence for the role of SESN2 in cancer proliferation (Supplementary Fig. 10a, b). Interestingly, we also found that ISRIB inhibited doxycycline-induced AKT (Ser473) phosphorylation (Fig. 3d), indicating that the ISR is required for AKT phosphorylation by the MSR as ISRIB is a known small-molecule integrated stress response (ISR) inhibitor that reverses the effects of eIF2α phosphorylation, which is an initiating event of ISR [53].

To determine whether AKT (Ser473) phosphorylation by the MSR involves SESN2, we generated two CRISPR-SESN2 knockout 8505C cell lines (CRISPR-SESN2-KO #1 and #2). Although doxycycline did not increase AKT (Ser473) phosphorylation in CRISPR-SESN2 #1 and #2 cells, it did increase AKT phosphorylation in the CRISPR-CTL cell line (Fig. 3e). Since mTORC2 phosphorylates AKT at Ser473 [23], we examined whether MSR-mediated AKT (Ser473) phosphorylation was increased in an mTORC2-dependent manner. Doxycycline-induced AKT (Ser473) phosphorylation was not reduced by silencing Raptor, a core component of mTORC1, but was abrogated by silencing Rictor, a core component of mTORC2 (Fig. 3f). Silencing Raptor or Rictor downregulated p-S6K (Thr389), indicating that p-S6K (Thr389) requires mTORC1 for MSR-induced mTORC2/AKT activation. Reducing mTORC1-induced S6K (Thr389) phosphorylation by silencing Raptor slightly increased p-AKT (Ser473) phosphorylation, potentially by alleviating the negative feedback effect of p-S6K on insulin receptor substrate 1 (IRS1) [54, 55]. Due to the complex crosstalk between mTORC2, AKT, mTORC1, and S6K, we examined the regulatory effects of the MSR on p-S6K (Thr389) via the mTORC2-AKT axis. Treating 8505C cells with doxycycline and A6730, an AKT inhibitor, downregulated MSR-mediated AKT (Ser473) and S6K (Thr389) phosphorylation (Supplementary Fig. 10c), suggesting that the MSR may induce mTORC2/AKT activation and S6K phosphorylation through a SESN2-dependent mechanism. mTORC2/AKT and mTORC1/S6K may also be synergistically activated via the MSR-induced upregulation of amino acid transporters.

The MSR-mTOR axis regulates tumour growth and aggressiveness in vivo

To validate the effect of the MSR on thyroid carcinogenesis in vivo, we created an orthotopic mouse model of thyroid cancer using CRISPR-SESN2-CTL and CRISPR-SESN2-KO cells. Consistent with our in vitro findings, orthotopic tumours were smaller in CRISPR-SESN2-KO mice than in CRISPR-SESN2-CTL mice (Fig. 3g, Supplementary Fig. 10d). Positron emission tomography with 2-deoxy-2-[fluorine-18] fluoro-D-glucose integrated with computed tomography (18F-FDG PET/CT) revealed decreased glucose metabolism in CRISPR-SESN2-KO tumours (Fig. 3g). In addition, p-AKT (Ser473) and p-S6K (Thr389) were downregulated in CRISPR-SESN2-KO tumours (Fig. 3h); however, PET/CT revealed no significant difference in ^{11}C-methionine uptake between the CRISPR-SESN2-KO and CRISPR-SESN2-CTL mice (Supplementary Fig. 10e), indicating that SESN2 plays no direct role in the uptake of large neutral amino acids.

We further validated the clinical significance of the MSR-mTOR-S6K axis by analysing TCGA-THCA-reverse phase protein array (RPPA) data divided into low and high p-S6K (Thr389) groups. GSEA of KEGG or Hallmark gene sets revealed that high S6K phosphorylation was associated with biosynthetic processes and cell proliferation-related pathways such as aminoacyl tRNA biosynthesis, DNA replication, and mTORC1 signalling (Supplementary Fig. 11a, b, Supplementary Tables 10 and 11). Conversely, high S6K (Thr389) phosphorylation was closely related to mitochondrial gene sets (Supplementary Fig. 11c, Supplementary Table 12). *HSPD1, ATF4, SESN2, GDF15, SLC7A5*, and *LARS* expression correlated positively with p-S6K (Thr389) but not total S6K, while p-AKT(S473) and p-AKT(T308) correlated positively with p-S6K (Thr389) (Supplementary Fig. 11d). We further examined the effect of high p-S6K (Thr389) on tumour aggressiveness using clinical data, finding that patients in the high p-S6K group was significantly older (Supplementary Fig. 12a) and that high p-S6K (Thr389) expression was related to aggressive clinicopathological features (Supplementary Fig. 12b–h) and a lower disease-free survival (Supplementary Fig. 12i). Collectively, these data suggest that the MSR-mTOR-S6K axis is important for the growth and aggressiveness of human thyroid cancer.

ISR-related ER stress is dependent on ^{mt}DNA

Thapsigargin, a non-competitive inhibitor of sarco/endoplasmic reticulum Ca ATPase (SERCA) induced ATF4/SESN2 like doxycycline (Fig. 4a). Moreover, the ER stressor tunicamycin increased mTOR, AKT, and S6K phosphorylation (Fig. 4b) and upregulated genes related to the MSR and the ER stress response, whereas doxycycline only induced MSR-related genes (Fig. 4c–e). Since ER stressors also induce the MSR, we examined the role of the MSR in ER stress-induced ISR by treating 8505C cells with ethidium bromide (EtBr) to deplete ^{mt}DNA (Supplementary Fig. 13a, b), as EtBr has been known to cause ^{mt}DNA depletion in a reproducible and dose-dependent manner in mammalian cells [56, 57]. After

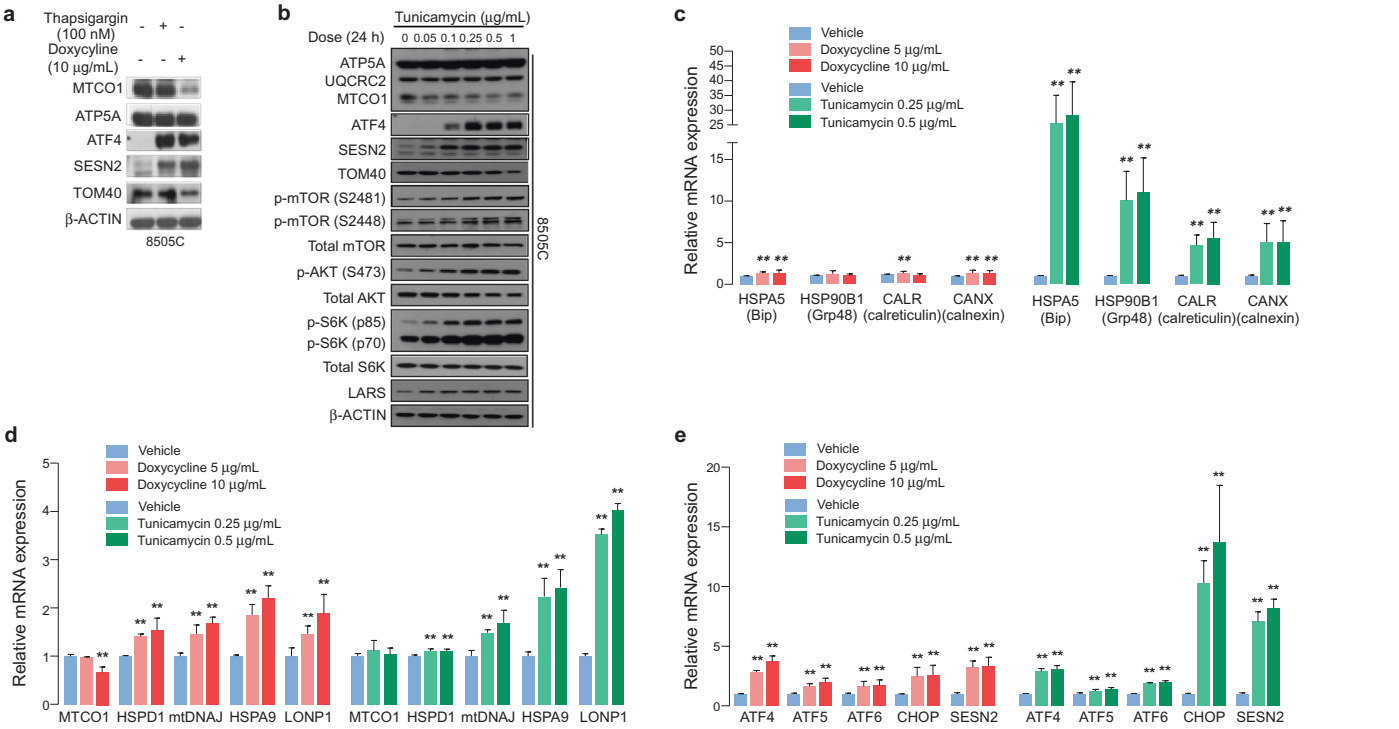

Fig. 4 Integrated stress response comparison between ^{mt}UPR and ER UPR. a OXPHOS, ATF4, and SESN2 expression in thapsigargin- or doxycycline-treated 8505C cells. **b** Changes in mTOR (Ser2481, Ser2448), AKT (Ser473), and S6K (Thr389) phosphorylation in tunicamycin-treated 8505C cells. **c** mRNA expression of ER stress response-related genes (HSPA5, HSP90B1, CALR, and CANX) in doxycycline- or tunicamycin-treated 8505C cells. **d** mRNA expression of MSR-related genes (MTCO1, HSPD1, mtDNAJ, HSPA9, and LONP1) in doxycycline- or tunicamycin-treated 8505C cells. **e** mRNA expression of ATFs (ATF4, 5, 6), CHOP, and SESN2 in doxycycline- or tunicamycin-treated 8505C cells. Data represent the mean ± SD of at least three independent experiments. $^{**}p < 0.01$. HSPA5, heat shock protein family A (Hsp70) member 5; HSP90B1, heat shock protein 90 beta family member 1; CALR, calreticulin; CANX, calnexin; mtDNAJ, DnaJ heat shock protein family (Hsp40); HSPA9, heat shock protein family A (Hsp70) member 9; CHOP, C/EBP homologous protein (DNA damage-inducible transcript 3 (DDIT3)).

5 days, doxycycline was unable to trigger mTOR phosphorylation or induce LAT1 and LARS1 (Fig. 5a). Increasing EtBr concentrations progressively decreased the expression of ^{mt}DNA-encoded genes (MTCO1) and reduced doxycycline-induced mTOR phosphorylation (Fig. 5b). mTOR phosphorylation and LARS1 induction by tunicamycin were also reversed in 8505C cells treated with EtBr (Fig. 5c), suggesting that ER stress-induced ISR requires ^{mt}DNA.

Since EtBr may induce the MSR, we classified thyroid cancer cell lines according to ^{mt}DNA copy number, finding that C643 cells had the lowest ^{mt}DNA copy number (Supplementary Fig. 13c). Interestingly, doxycycline failed to induce ATF4/SESN2, LAT1, or LARS1 in these cells (Supplementary Fig. 13d, e), whereas TPC1 and 8505 C cells (similar ^{mt}DNA copy numbers) responded similarly to doxycycline (Supplementary Fig. 13f, g). In TCGA-THCA, ^{mt}DNA copy number correlated significantly with the MSR and AKT-mTOR signalling (Supplementary Fig. 14a) and ER stress markers were downregulated in most PTC samples (Supplementary Fig. 14b). Thus, we postulated that the MSR is clinically relevant and that ^{mt}DNA is essential in mitochondria- and ER-induced ISR.

BRAF^{V600E}-induced MYC activation requires ^{mt}DNA to amplify the MSR

Since ^{mt}DNA is crucial for the ISR, we investigated the underlying regulatory mechanism. First, we tested whether the BRAF^{V600E} mutation, the most common driver mutation in PTC, could directly induce the MSR as a mitochondrial stress inducer. Notably, oncogenes such as RAS proto-oncogene, GTPase (RAS), AKT/PKB, hypoxia-inducible factor (HIF), and BRAF^{V600E} have been known to inhibit mitochondrial respiration and promote glycolysis, thereby generating aerobic glycolysis, a phenomenon termed "the Warburg effect" [58, 59]. Moreover, BRAFV600E was more frequently detected in non-ovPTC harbouring high ^{mt}DNA/nDNA ratio (Table 1). Infecting immortalized normal thyroid follicular cells (Nthy-ori 3–1) with mutant BRAF (BRAF^{V600E}) lentivirus increased the ^{mt}DNA copy number compared to wild-type BRAF (BRAF^{WT}; Fig. 5d). This effect was synergistic with MYC, as identified by GSEA of PTC with high ^{mt}DNA copy number (Fig. 1h). BRAF^{V600E} and ERK phosphorylation decreased MTCO1 and induced the MSR, which was reversed by PLX4032 (BRAF^{V600E} inhibitor) and SCH772984 (ERK inhibitor; Fig. 5e, Supplementary Fig. 15a). Since ISRIB reversed all aspects of doxycycline-induced MSR except for ^{mt}DNA-encoded genes (Fig. 5f), we evaluated whether ISRIB affected ^{mt}DNA copy number. ISRIB countered the effects of doxycycline-induced MSR on amino acid metabolism, mTOR signalling, and UPR (PERK signalling, ATF and MYC transactivation; Fig. 6a). Consistently, SCH772984 and ISRIB significantly decreased ^{mt}DNA copy number upregulation by BRAF^{V600E} (Fig. 6b). However, SCH772984 and ISRIB did not affect ^{mt}DNA copy number upregulation by MYC (Supplementary Fig. 15b), even when co-transfected with BRAF^{V600E} (Fig. 6c), indicating that MYC is the final effector of increased ^{mt}DNA copy number. Indeed, MYC silencing (shMYC) abolished the increase in ^{mt}DNA copy number induced by BRAF^{V600E} or doxycycline (Fig. 6d). Doxycycline-induced MSR increased MYC expression in a similar manner to BRAF^{V600E} and MYC silencing almost abolished the expression and phosphorylation of major MSR components (Fig. 6e, Supplementary Fig. 15c), indicating that MSR and MYC are co-dependent. Accordingly, MYC expression and eIF2α and mTOR phosphorylation were decreased in Rho0 cells generated using mitochondrial uracil-DNA glycosylase (UNG1; Supplementary Fig. 15d, Fig. 6f). Taken together, our data indicate that oncogenic

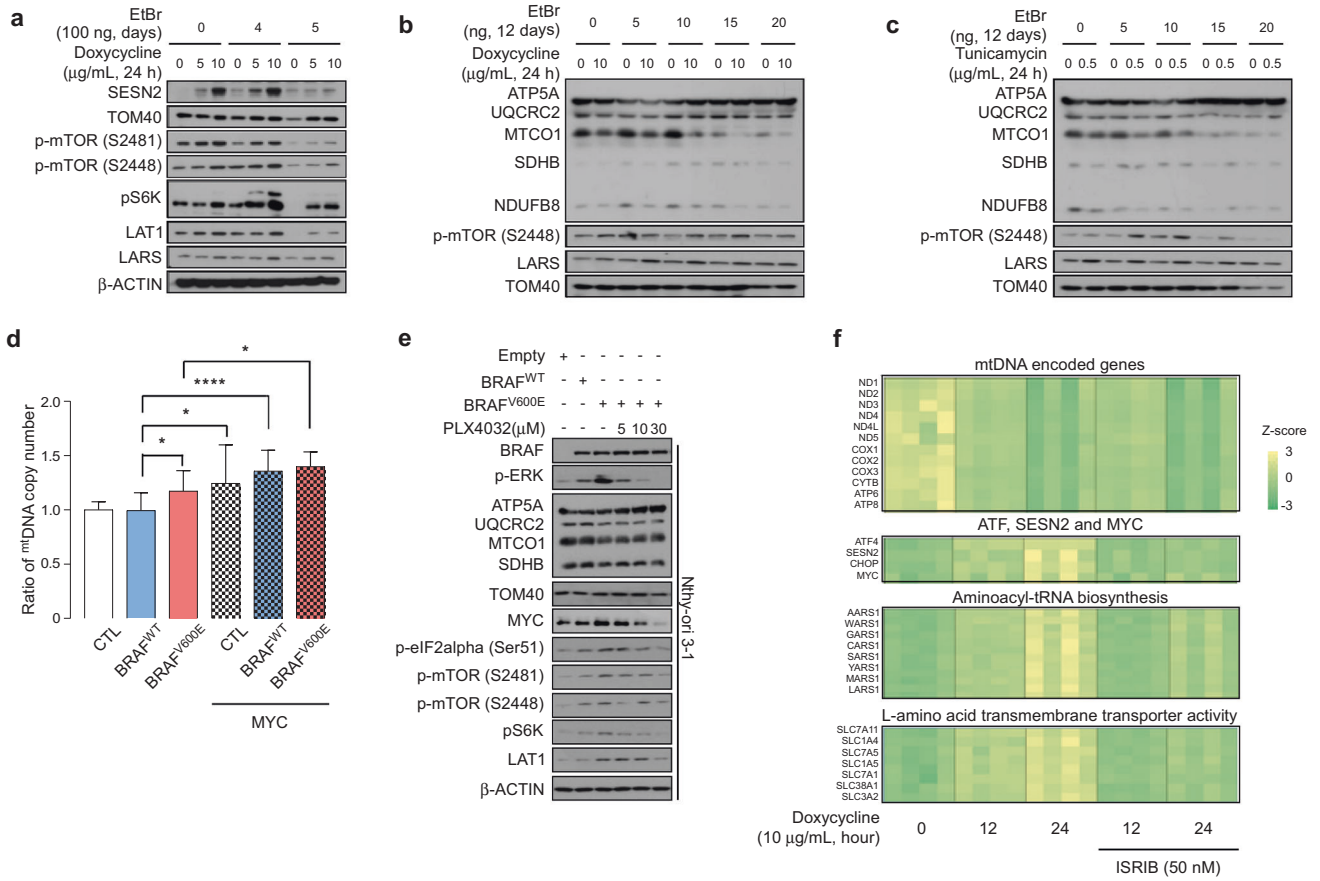

Fig. 5 ^{mt}DNA depletion affects the integrated stress response from mitochondria and the ER. a Effect of ^{mt}DNA depletion by 100 ng/mL EtBr on SESN2, TOM40, LAT1, and LARS protein expression and mTOR (Ser2481 and Ser2448) and S6K (Thr389) phosphorylation in doxycycline-treated 8505C cells. **b**, **c** Effect of ^{mt}DNA depletion on the protein expression or phosphorylation of OXPHOS (ATP5A, UQCRC2, MTCO1, SDHB, NDUFB8), mTOR (Ser2448), LARS, and TOM40 in 8505C cells treated with doxycycline (**b**) or tunicamycin (**c**). **d** ^{mt}DNA copy number alterations induced by BRAF^{V600E} and MYC. **e** Effect of BRAF^{V600E} on MSR via kinase activity. **f** Heat-map of changes in MSR-related gene expression in 8505C cells treated with doxycycline alone or with ISRIB. *$p < 0.05$, ****$p < 0.0001$. EtBr ethidium bromide.

BRAF^{V600E} induces MSR via an ERK and ^{mt}DNA-dependent mechanism and that MYC transactivation may increase ^{mt}DNA copy number to amplify the MSR (Fig. 6g).

DISCUSSION

Metabolic remodelling is an essential process that provides energy to support cancer cell growth and division. Decades ago, cancer cells were found to ferment glucose even in the presence of oxygen, suggesting that mitochondrial respiration defects underlie cancer development [60, 61]. However, more recent studies have demonstrated that the genetic events that promote aerobic glycolysis do not impair mitochondrial gene expression [58] and that mitochondrial biogenesis and quality control are often upregulated in cancer and coupled with mitochondrial stress [62]. Consistently, OXPHOS protein expression does not decrease uniformly in PTC. In fact, we postulated that an increased ^{mt}DNA copy number could proportionally unbalance ^{mt}DNA and ^{n}DNA, triggering the ^{mt}UPR. Cross-sectional analyses from this study revealed a relationship between ^{mt}DNA copy number and the expression of mitochondrial stress-related genes, such as HSPD1, LONP1, and GDF15. Moreover, our analyses suggested that tumour cells may experience more stress than normal cells and thus require a more robust retrograde mechanism to regulate mitochondrial stress and maintain metabolic homoeostasis.

Although we focused on the regulation of ^{mt}UPR by oncogenic signalling in this study, diverse mitochondrial stressors (oxidative stress, complex inhibition) may also be linked to the ISR and mTOR signalling. Multi-omics approaches have recently indicated that compounds that alter mitochondrial function activate the ISR, allowing the main effector, ATF4, to promote the expression of specific cytoprotective genes that reprogramme cellular metabolism toward the synthesis of key metabolites [18]. Here, we found that the MSR induced by doxycycline, FCCP, or rotenone consistently upregulated ATF4, leading to SESN2 accumulation in cancer cells. SESN2 contains an ATF4 binding motif, suggesting that SESN2 is induced by MSR-mediated ATF4 transactivation [46]. Although SESN2 can exert tumour-suppressive effects by inhibiting mTORC1 to restrict protein synthesis upon amino acid deprivation or unfolded protein accumulation, thereby protecting cells from nutrient crisis or ER stress, SESNs are highly expressed in many cancers [63]; however, their molecular mechanism in tumour progression remain largely unclear [64–66]. Here, we demonstrated that SESN2 plays an essential role in MSR-induced AKT phosphorylation. ^{mt}DNA is an essential component of mitochondrial and ER-induced ISR, as confirmed in our experiments using Rho0 cells. Interestingly, the oncogene BRAF^{V600E} increased ^{mt}DNA copy number via the downstream transcription factor, MYC, suggesting that oncogenic signalling can induce the ISR. Similarly, the mitochondrial stress inducer, doxycycline, increased MYC expression and ^{mt}DNA copy number in an ISR-dependent manner. Since cancer cells experience many types of metabolic stress (hypoxia, oxidative stress, nutrient deprivation), this bi-directional loop may be an important mitochondrial survival strategy [11].

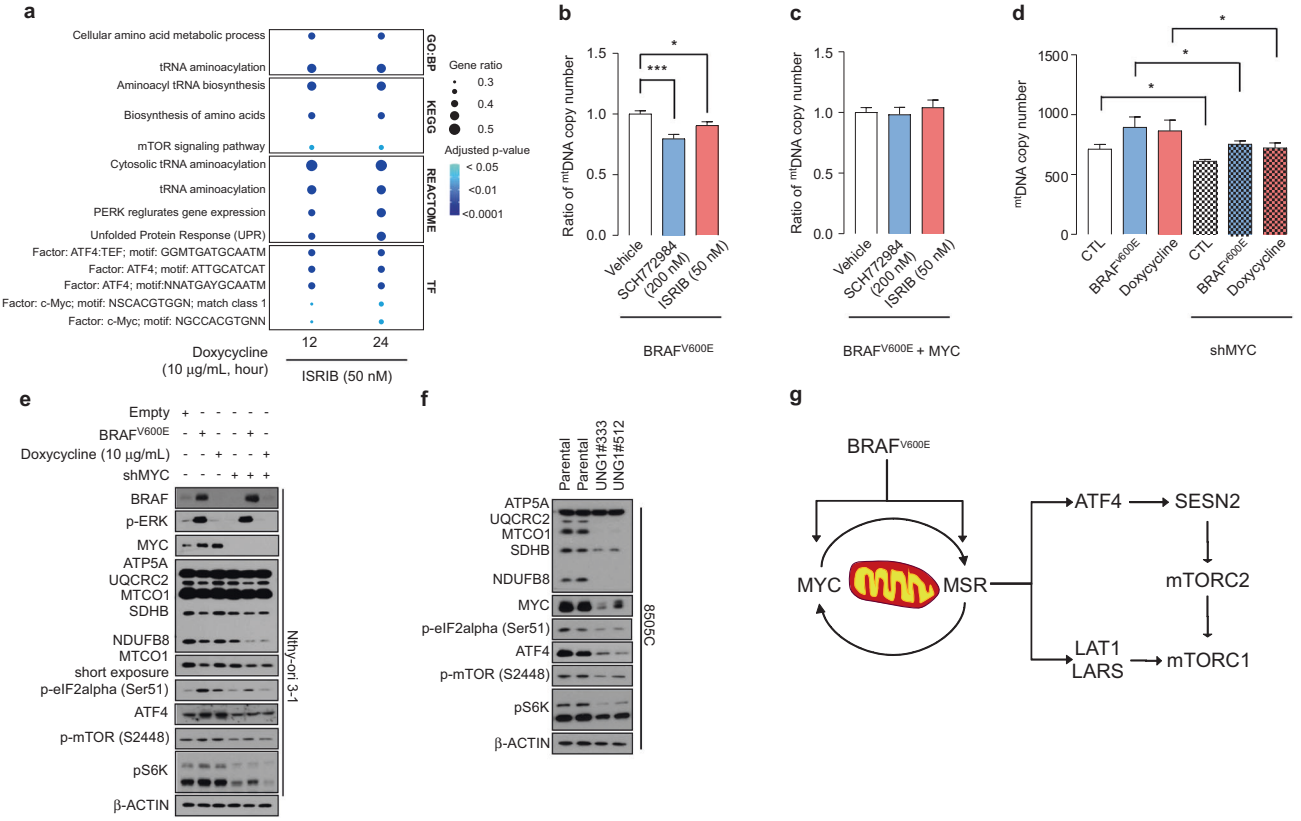

Fig. 6 MYC transactivation is a critical regulator of positive feedback loop formation in the MSR. a Dot plot of significantly enriched GO (BP biological process), KEGG, Reactome (REACTOME), and transcription factor (TF) terms in response to the doxycycline with ISRIB of doxycycline alone in 8505 C cells. Dot size represents gene ratio and colour represents adjusted *p* value. **b** ^{mt}DNA copy number alterations by BRAF^{V600E} via ERK and ISR. BRAFV600E lentivirus infected Nthy-ori-3-1 cells were treated with SCH772984 (ERK inhibitor, 200 nM, 24 h) and ISRIB (ISR inhibitor, 50 nM, 24 h). **c** ^{mt}DNA copy number alterations by BRAF^{V600E} via MYC. **d** The effect of MYC silencing on the changes in ^{mt}DNA copy number induced by BRAF^{V600E} or doxycycline. **e** Effect of MYC silencing on the ISR induced by BRAF^{V600E} or doxycycline. **f** Effect of mtDNA depletion by stable UNG1 expression on MSR. **g** Schematic summary of this study. All experiments were performed at least three times. $*p < 0.05$, $**p < 0.01$, $***p < 0.001$, $****p < 0.0001$. UNG1 uracil-DNA glycosylase.

The MSR stimulates the synthesis of specific mitochondrial proteins by counteracting the effect of mitochondrial stress on cellular homoeostasis [13, 15]. In *C. elegans* and *D. melanogaster*, mitochondrial proteotoxic stress activates the ^{mt}UPR, a typical feature of the MSR that promotes the transcription of proteases, chaperones, and metabolic enzymes which restore mitochondrial function and cellular homoeostasis [12–15]. In tumour cells, the MSR is not limited to mitochondrial quality control and restoration. Here, GSEA of high ^{mt}DNA copy number and HSPD1 showed a consistent increase in overall amino acid metabolism, MYC targets, and mTOR signalling, suggesting that tumour cells exploit evolutionarily conserved mechanisms to overcome mitochondrial stress, stimulate protein synthesis, and sustain tumour growth. In addition, the MSR modulated amino acid metabolism in cancer cells. Previous studies have shown that SESNs inhibit Rag GTPases that are essential for mTORC1 activity by inhibiting GATOR2 [67, 68], which is disrupted by Leu [47, 48]. GSEA indicated that the MSR was related to amino acid biosynthesis, transporters, and aminoacyl tRNA biosynthesis. In particular, the MSR was important for LAT1 and LARS induction in Leu metabolism and may reprogram amino acid metabolism to avoid SESN2-mediated mTORC1 inhibition. Furthermore, increased Leu uptake could promote MSR-mediated mTORC1 activation. The MSR also directly activates mTORC2-AKT signalling and thereby increases S6K (Thr389) phosphorylation. AKT is a key oncogenic signalling molecule that is activated in most cancers, including thyroid cancer, and integrates growth factor responses with cell survival, proliferation, and bioenergetics [69]. In addition, AKT is involved in tumour adaptation to hypoxia [70] and nutrient depletion [44]. Here, we revealed that mitochondrial stress, as a cell-autonomous stress response, regulates cancer progression by activating AKT in the absence of canonical genetic or genomic alterations, thereby facilitating S6K phosphorylation. These adaptive processes were critical for tumour cell growth in our orthotopic mouse model of thyroid cancer and correlated with aggressive tumour behaviour, poor clinical risk scores, and a shorter DFS. Consequently, this mechanism could be used to predict poor prognosis in patients with thyroid cancer.

In conclusion, we demonstrated that mitochondrial stress drives tumour progression via the MSR-mediated reprogramming of amino acid metabolism and activation of SESN2-mTORC2-AKT/S6K signalling. We also validated the clinical significance of this cell-autonomous regulatory mechanism on unfavourable outcomes in patients with thyroid cancer. Thus, major components of this pathway could be promising diagnostic biomarkers for aggressive thyroid cancer and ISRIB, a potent ISR inhibitor, could be a potential therapeutic agent.

MATERIALS/SUBJECTS AND METHODS

Detailed information for key resources and methods are provided in Supplementary Information.

Experimental design

To investigate the role of mitochondrial stress response in cancer cell biology such as growth signalling and amino acid metabolism, we collected formalin fixed paraffin-embedded tissues of human papillary thyroid cancer ($n = 208$) with paired normal tissues including oncocytic variant papillary thyroid cancer ($n = 11$) according to their histologic diagnosis. Sample size was determined by tissue availability. Identifying the relationship of ^{mt}DNA/^{n}DNA ratio with mitochondrial stress response, gene set enrichment analysis using TCGA-THCA and our own transcriptome data ($n = 292$) was performed.

To verify the signal propagation generated by mitochondrial stress response, 8505C cells with or without doxycycline and a small-molecule ISR inhibitor (ISRIB), were subjected to RNA sequencing. Diverse mitochondrial stress inducers such as carbonyl cyanide-4-(trifluoromethoxy) phenylhydrazone (FCCP), and rotenone and various cancer cell lines such as BCPAP, TPC1, FTC133, SW1736, CAL62, HTH83, and C643 were used for the validation experiments.

To prove the direct regulation of SESN2 on mTOR signalling, CRISPR/Cas9 genetically modified cells targeting SESN2 were generated and used for orthotopic xenograft mouse models. Sample size varied depending on animal availability; however, seven mice were analysed for ^{18}F-FDG-PET and ten mice were subjected to ^{11}C-Methionine-PET.

To investigate the relationship of mitochondrial stress on mTOR and amino acid metabolism, we performed extensive correlative analyses and conducted qRT-PCR and western blot analysis to prove the identified correlation. Using EtBr and mutant Y147A human uracil-DNA glycosylases (mtUNG1) by lentiviral transduction, we generated Rho0 cells, which are devoid of mtDNA. For cell-based assays, at least three biological replicates per group were studied.

Patients and specimens

Human thyroid cancer and matched contralateral normal fresh tissue samples were obtained from patients who underwent thyroidectomy for papillary thyroid cancer (PTC) at Yonsei Cancer Center (Seoul, South Korea) between April 2014 and December 2017. All samples were frozen in liquid nitrogen and stored at −80 °C prior to analysis. All patients provided written informed consent. The study protocols were approved by the Institutional Review Board of Severance Medical Center (Seoul, Korea).

Orthotopic xenograft mouse model

Five-week-old male athymic nude BALB/c mice were obtained from Orientbio (Seongnam-si, Korea). The left and right thyroid glands were injected orthotopically with CRISPR-SESN2 and CRISPR-CTL cells (1×10^5 cells in 5 µL phosphate-buffered saline, PBS, #P3813, Sigma-Aldrich), respectively, using a 25 µL syringe (Hamilton, Reno, NV, USA). ^{18}F-FDG and ^{11}C-MET were synthesised in-house using a Cyclone 18/9 cyclotron (IBA - Radiopharma Solutions, Reston, VA). Dynamic ^{18}F-FDG or ^{11}C-MET PET were performed using an Inveon™ Dedicated Micro PET (SIEMENS Medical Systems, Erlangen, Germany) for 1 h, with intravenous injections of 200 µCi/0.1 mL ^{18}F-FDG or 400 µCi/0.2 mL ^{11}C-MET. CT was performed using an NFR Polaris G90 Micro CT (Nano Focus Ray, Jeonju-si, South Korea). Before FDG PET/CT, mice were fasted for a minimum of 12 h. Short-acting isoflurane anaesthesia (2% isoflurane, 98% air) was used throughout the study. After imaging, the mice were sacrificed and tumour tissues extracted for western blot analysis.

All images were analysed using Amide's Medical Image Data Examiner (AMIDE, http://amide.sourceforge.net/index.html). PET data were arranged into sinograms with Fourier 2D rebinning and reconstructed to generate 3D DICOM images using the Ordered Subset Expectation Maximization (OSEM3D) algorithm. After qualitative assessment, the region of interest was drawn manually to cover the entire tumour within the tomographic planes. Tumour tracer uptake (standardised uptake value; SUV) was assessed as follows: SUV = tissue activity concentration (Bq/mL)/injected dose (Bq)/body weight (g). PET and CT images were fused using MIM v6.6.7 (MIM Software, Cleveland, OH, USA). All animal experiments were approved by the Committee for Ethics in Animal Experiments of Yonsei University College of Medicine. All mice were handled according to the care and use of laboratory animal guidelines of the Department of Laboratory Animal Resources, Yonsei University College of Medicine.

DATA AVAILABILITY

The datasets generated during and/or analysed during this study are available from the corresponding author on reasonable request.

REFERENCES

1. Ward PS, Thompson CB. Metabolic reprogramming: a cancer hallmark even warburg did not anticipate. Cancer Cell. 2012;21:297–308.
2. Vander Heiden MG, Cantley LC, Thompson CB. Understanding the Warburg effect: the metabolic requirements of cell proliferation. Science. 2009;324:1029–33.
3. Zaugg K, Yao Y, Reilly PT, Kannan K, Kiarash R, Mason J, et al. Carnitine palmitoyltransferase 1C promotes cell survival and tumor growth under conditions of metabolic stress. Genes Dev. 2011;25:1041–51.
4. Choo AY, Kim SG, Vander Heiden MG, Mahoney SJ, Vu H, Yoon S-O, et al. Glucose addiction of TSC null cells is caused by failed mTORC1-dependent balancing of metabolic demand with supply. Mol Cell. 2010;38:487–99.
5. Gao P, Tchernyshyov I, Chang T-C, Lee Y-S, Kita K, Ochi T, et al. c-Myc suppression of miR-23a/b enhances mitochondrial glutaminase expression and glutamine metabolism. Nature. 2009;458:762.
6. Wise DR, DeBerardinis RJ, Mancuso A, Sayed N, Zhang X-Y, Pfeiffer HK, et al. Myc regulates a transcriptional program that stimulates mitochondrial glutaminolysis and leads to glutamine addiction. Proc Natl Acad Sci USA 2008;105:18782–7.
7. Vyas S, Zaganjor E, Haigis MC. Mitochondria and cancer. Cell. 2016;166:555–66.
8. Chandel NS. Evolution of mitochondria as signaling organelles. Cell Metab. 2015;22:204–6.
9. Quirós PM, Mottis A, Auwerx J. Mitonuclear communication in homeostasis and stress. Nat Rev Mol Cell Biol. 2016;17:213.
10. Matilainen O, Quirós PM, Auwerx J. Mitochondria and epigenetics–crosstalk in homeostasis and stress. Trends Cell Biol. 2017;27:453–63.
11. O'Malley J, Kumar R, Inigo J, Yadava N, Chandra D. Mitochondrial stress response and cancer. Trends Cancer. 2020;6:688–701.
12. Durieux J, Wolff S, Dillin A. The cell-non-autonomous nature of electron transport chain-mediated longevity. Cell. 2011;144:79–91.
13. Yoneda T, Benedetti C, Urano F, Clark SG, Harding HP, Ron D. Compartment-specific perturbation of protein handling activates genes encoding mitochondrial chaperones. J Cell Sci. 2004;117:4055–66.
14. Nargund AM, Pellegrino MW, Fiorese CJ, Baker BM, Haynes CM. Mitochondrial import efficiency of ATFS-1 regulates mitochondrial UPR activation. Science. 2012;337:587–90.
15. Houtkooper RH, Mouchiroud L, Ryu D, Moullan N, Katsyuba E, Knott G, et al. Mitonuclear protein imbalance as a conserved longevity mechanism. Nature. 2013;497:451.
16. D'Amico D, Sorrentino V, Auwerx J. Cytosolic proteostasis networks of the mitochondrial stress response. Trends Biochem Sci. 2017;42:712–25.
17. Harding HP, Zhang Y, Zeng H, Novoa I, Lu PD, Calfon M, et al. An integrated stress response regulates amino acid metabolism and resistance to oxidative stress. Mol Cell. 2003;11:619–33.
18. Quiros PM, Prado MA, Zamboni N, D'Amico D, Williams RW, Finley D, et al. Multi-omics analysis identifies ATF4 as a key regulator of the mitochondrial stress response in mammals. J Cell Biol. 2017;216:2027–45.
19. Tyynismaa H, Carroll CJ, Raimundo N, Ahola-Erkkilä S, Wenz T, Ruhanen H, et al. Mitochondrial myopathy induces a starvation-like response. Hum Mol Genet. 2010;19:3948–58.
20. Martínez-Reyes I, Sánchez-Aragó M, Cuezva JM. AMPK and GCN2–ATF4 signal the repression of mitochondria in colon cancer cells. Biochem J. 2012;444:249–59.
21. Hanahan D, Weinberg RA. Hallmarks of cancer: the next generation. Cell. 2011;144:646–74.
22. Hanahan D, Weinberg RA. The hallmarks of cancer. Cell. 2000;100:57–70.
23. Sarbassov DD, Guertin DA, Ali SM, Sabatini DM. Phosphorylation and regulation of Akt/PKB by the rictor-mTOR complex. Science. 2005;307:1098–101.

24. Zhou Q, Liu C, Liu W, Zhang H, Zhang R, Liu J, et al. Rotenone induction of hydrogen peroxide inhibits mTOR-mediated S6K1 and 4E-BP1/eIF4E pathways, leading to neuronal apoptosis. Toxicol Sci. 2015;143:81–96.
25. Peng M, Ostrovsky J, Kwon YJ, Polyak E, Licata J, Tsukikawa M, et al. Inhibiting cytosolic translation and autophagy improves health in mitochondrial disease. Hum Mol Genet. 2015;24:4829–47.
26. Johnson SC, Yanos ME, Kayser EB, Quintana A, Sangesland M, Castanza A, et al. mTOR inhibition alleviates mitochondrial disease in a mouse model of Leigh syndrome. Science. 2013;342:1524–8.
27. Zheng X, Boyer L, Jin M, Kim Y, Fan W, Bardy C, et al. Alleviation of neuronal energy deficiency by mTOR inhibition as a treatment for mitochondria-related neurodegeneration. Elife. 2016;5:e13378.
28. Nacarelli T, Azar A, Sell C. Aberrant mTOR activation in senescence and aging: a mitochondrial stress response? Exp Gerontol. 2015;68:66–70.
29. Steffen KK, Dillin A. A ribosomal perspective on proteostasis and aging. Cell Metab. 2016;23:1004–12.
30. Ding L, Bailey MH, Porta-Pardo E, Thorsson V, Colaprico A, Bertrand D, et al. Perspective on oncogenic processes at the end of the beginning of cancer genomics. Cell. 2018;173:305–320.e310.
31. Bailey MH, Tokheim C, Porta-Pardo E, Sengupta S, Bertrand D, Weerasinghe A, et al. Comprehensive characterization of cancer driver genes and mutations. Cell. 2018;173:371–385.e318.
32. Taylor AM, Shih J, Ha G, Gao GF, Zhang X, Berger AC, et al. Genomic and functional approaches to understanding cancer aneuploidy. Cancer Cell. 2018;33:676–89.e673.
33. Zhang Y, Kwok-Shing NgP, Kucherlapati M, Chen F, Liu Y, Tsang YH, et al. A Pan-cancer proteogenomic atlas of PI3K/AKT/mTOR pathway alterations. Cancer Cell. 2017;31:820–832.e823.
34. Liu J, Lichtenberg T, Hoadley KA, Poisson LM, Lazar AJ, Cherniack AD, et al. An Integrated TCGA Pan-cancer clinical data resource to drive high-quality survival outcome analytics. Cell. 2018;173:400–416.e411.
35. Sanchez-Vega F, Mina M, Armenia J, Chatila WK, Luna A, La KC, et al. Oncogenic signaling pathways in The Cancer Genome Atlas. Cell. 2018;173:321–337.e310.
36. Peng X, Chen Z, Farshidfar F, Xu X, Lorenzi PL, Wang Y, et al. Molecular characterization and clinical relevance of metabolic expression subtypes in human cancers. Cell Rep. 2018;23:255–269.e254.
37. Alexandrov LB, Nik-Zainal S, Wedge DC, Aparicio SA, Behjati S, Biankin AV, et al. Signatures of mutational processes in human cancer. Nature. 2013;500:415–21.
38. Agrawal N, Akbani R, Aksoy BA, Ally A, Arachchi H, Asa SL, et al. Integrated genomic characterization of papillary thyroid carcinoma. Cell. 2014;159:676–90.
39. Bao X, Zhang J, Huang G, Yan J, Xu C, Dou Z, et al. The crosstalk between HIFs and mitochondrial dysfunctions in cancer development. Cell Death Dis. 2021;12:215.
40. Porporato PE, Filigheddu N, Pedro JMB, Kroemer G, Galluzzi L. Mitochondrial metabolism and cancer. Cell Res. 2018;28:265–80.
41. Ishida S, Andreux P, Poitry-Yamate C, Auwerx J, Hanahan D. Bioavailable copper modulates oxidative phosphorylation and growth of tumors. Proc Natl Acad Sci USA 2013;110:19507–12.
42. Yi HS, Chang JY, Shong M. The mitochondrial unfolded protein response and mitohormesis: a perspective on metabolic diseases. J Mol Endocrinol. 2018;61:R91–R105.
43. Moullan N, Mouchiroud L, Wang X, Ryu D, Williams EG, Mottis A, et al. Tetracyclines disturb mitochondrial function across eukaryotic models: a call for caution in biomedical research. Cell Rep. 2015;10:1681–91.
44. Byun J-K, Choi Y-K, Kim J-H, Jeong JY, Jeon H-J, Kim M-K, et al. A positive feedback loop between sestrin2 and mTORC2 is required for the survival of glutamine-depleted lung cancer cells. Cell Rep. 2017;20:586–99.
45. Kowalsky AH, Namkoong S, Mettetal E, Park HW, Kazyken D, Fingar DC, et al. The GATOR2-mTORC2 axis mediates Sestrin2-induced AKT Ser/Thr kinase activation. J Biol Chem. 2020;295:1769–80.
46. Garaeva AA, Kovaleva IE, Chumakov PM, Evstafieva AG. Mitochondrial dysfunction induces SESN2 gene expression through Activating Transcription Factor 4. Cell Cycle. 2016;15:64–71.
47. Wolfson RL, Chantranupong L, Saxton RA, Shen K, Scaria SM, Cantor JR, et al. Sestrin2 is a leucine sensor for the mTORC1 pathway. Science. 2016;351:43–48.
48. Saxton RA, Knockenhauer KE, Wolfson RL, Chantranupong L, Pacold ME, Wang T, et al. Structural basis for leucine sensing by the Sestrin2-mTORC1 pathway. Science. 2016;351:53–58.
49. Ringel MD, Hayre N, Saito J, Saunier B, Schuppert F, Burch H, et al. Overexpression and overactivation of Akt in thyroid carcinoma. Cancer Res. 2001;61:6105–11.
50. Vasko V, Espinosa AV, Scouten W, He H, Auer H, Liyanarachchi S, et al. Gene expression and functional evidence of epithelial-to-mesenchymal transition in papillary thyroid carcinoma invasion. Proc Natl Acad Sci USA 2007;104:2803–8.
51. Knippler CM, Saji M, Rajan N, Porter K, La Perle K, Ringel MD. MAPK- and AKT-activated thyroid cancers are sensitive to group I PAK inhibition. Endocr Relat Cancer. 2019;26:699–712.
52. Xing M. Molecular pathogenesis and mechanisms of thyroid cancer. Nat Rev Cancer. 2013;13:184–99.
53. Matts RL, Levin DH, London IM. Effect of phosphorylation of the alpha-subunit of eukaryotic initiation factor 2 on the function of reversing factor in the initiation of protein synthesis. Proc Natl Acad Sci USA 1983;80:2559–63.
54. Zhang J, Gao Z, Yin J, Quon MJ, Ye J. S6K directly phosphorylates IRS-1 on Ser270 to promote insulin resistance in response to TNF-α signaling through IKK2. J Biol Chem. 2008;283:35375–82.
55. Um SH, Frigerio F, Watanabe M, Picard F, Joaquin M, Sticker M, et al. Absence of S6K1 protects against age- and diet-induced obesity while enhancing insulin sensitivity. Nature. 2004;431:200–5.
56. King MP, Attardi G. Human cells lacking mtDNA: repopulation with exogenous mitochondria by complementation. Science. 1989;246:500–3.
57. Yu M, Shi Y, Wei X, Yang Y, Zhou Y, Hao X, et al. Depletion of mitochondrial DNA by ethidium bromide treatment inhibits the proliferation and tumorigenesis of T47D human breast cancer cells. Toxicol Lett. 2007;170:83–93.
58. Hsu PP, Sabatini DM. Cancer cell metabolism: Warburg and beyond. Cell. 2008;134:703–7.
59. Lee MH, Lee SE, Kim DW, Ryu MJ, Kim SJ, Kim SJ, et al. Mitochondrial localization and regulation of BRAFV600E in thyroid cancer: a clinically used RAF inhibitor is unable to block the mitochondrial activities of BRAFV600E. J Clin Endocrinol Metab. 2011;96:E19–30.
60. Warburg O. On the origin of cancer cells. Science. 1956;123:309–14.
61. Warburg O. On respiratory impairment in cancer cells. Science. 1956;124:269–70.
62. Mathupala SP, Ko YH, Pedersen PL. The pivotal roles of mitochondria in cancer: Warburg and beyond and encouraging prospects for effective therapies. Biochim Biophys Acta. 2010;1797:1225–30.
63. Budanov AV, Shoshani T, Faerman A, Zelin E, Kamer I, Kalinski H, et al. Identification of a novel stress-responsive gene Hi95 involved in regulation of cell viability. Oncogene. 2002;21:6017.
64. Park H-W, Park H, Ro S-H, Jang I, Semple IA, Kim DN, et al. Hepatoprotective role of Sestrin2 against chronic ER stress. Nat Commun. 2014;5:4233.
65. Peng M, Yin N, Li MO. Sestrins function as guanine nucleotide dissociation inhibitors for Rag GTPases to control mTORC1 signaling. Cell. 2014;159:122–33.
66. Ye J, Palm W, Peng M, King B, Lindsten T, Li MO, et al. GCN2 sustains mTORC1 suppression upon amino acid deprivation by inducing Sestrin2. Genes Dev. 2015;29:2331–6.
67. Chantranupong L, Wolfson RL, Orozco JM, Saxton RA, Scaria SM, Bar-Peled L, et al. The Sestrins interact with GATOR2 to negatively regulate the amino-acid-sensing pathway upstream of mTORC1. Cell Rep. 2014;9:1–8.
68. Parmigiani A, Nourbakhsh A, Ding B, Wang W, Kim YC, Akopiants K, et al. Sestrins inhibit mTORC1 kinase activation through the GATOR complex. Cell Rep. 2014;9:1281–91.
69. Manning BD, Cantley LC. AKT/PKB signaling: navigating downstream. Cell. 2007;129:1261–74.
70. Chae YC, Vaira V, Caino MC, Tang H-Y, Seo JH, Kossenkov AV, et al. Mitochondrial Akt regulation of hypoxic tumor reprogramming. Cancer Cell. 2016;30:257–72.

ACKNOWLEDGEMENTS

Anti-SESN2 polyclonal antibodies and SESN2 plasmids were provided by Prof. Soo Han Bae (Severance Biomedical Science Institute and Yonsei Biomedical Research Institute, Yonsei University College of Medicine, 03722, Seoul, South Korea). We thank Ji Young Kim, Hee Chang Yu, Hoyoung Kim, and Hwa Young Lee for their excellent technical support.

AUTHOR CONTRIBUTIONS

Conceptualization: JA, JL, and YSJ; Methodology: WKL, SP, SGL, SJ, GL, DR, KS, and JA; Investigation: WKL, SP, SGL, SJ, GL, and DR; Visualization: WKL, SP, SGL, SJ, and GL; Funding acquisition: KS, JA, JL, and YSJ; Project administration: JL and YSJ; Supervision: KS, JA, JL, and YSJ. Writing – original draft: WKL and SP; Writing – review & editing: WKL, SP, SGL, KS, JA, JL, and YSJ.

FUNDING

We received funding from the National Research Foundation of Korea grant, funded by the Korean government NRF-2018R1A2B6004179 and NRF-2021R1H1A2012035 (YSJ); NRF-2020R1A2C1006047 (JL); NRF-2020R1I1A1A01069524 (SP); National Research Foundation of Korea GRL grant NRF-2017K1A1A2013124 (JA); École Polytechnique Fédérale de Lausanne (JA and KS); European Research Council ERC-AdG-787702 (JA); Swiss Cancer Research KFS-4226-08-2017 (KS); and Swiss National Science Foundation, Sinergia CRSII3_160798 (KS).

COMPETING INTERESTS

The authors declare no competing interests.

ADDITIONAL INFORMATION

Supplementary information The online version contains supplementary material available at https://doi.org/10.1038/s41388-022-02484-7.

Correspondence and requests for materials should be addressed to Jandee Lee or Young Suk Jo.

Reprints and permission information is available at http://www.nature.com/reprints

Publisher's note Springer Nature remains neutral with regard to jurisdictional claims in published maps and institutional affiliations.

Springer Nature or its licensor holds exclusive rights to this article under a publishing agreement with the author(s) or other rightsholder(s); author self-archiving of the accepted manuscript version of this article is solely governed by the terms of such publishing agreement and applicable law.